Amino acid substitutions in the human homomeric β3 GABAA receptor that enable activation by GABA

Gottschald Chiodi, Carla; Baptista-Hon, Daniel; Hunter, William; Hales, Tim

Published in:
Journal of Biological Chemistry

DOI:
10.1074/jbc.RA118.006229

Publication date:
2019

Document Version
Peer reviewed version

Amino acid substitutions in the human homomeric β_3 $GABA_A$ receptor that enable activation by GABA

Carla Gottschald Chiodi[1], Daniel T. Baptista-Hon[2], William N. Hunter[1] and Tim G. Hales[2]

[1] Biological Chemistry and Drug Discovery, School of Life Sciences, University of Dundee, Dundee, DD1 5EH, UK.
[2] The Institute of Academic Anaesthesia, Division of Systems Medicine, School of Medicine, Ninewells Hospital, University of Dundee, Dundee, DD1 9SY, UK.

Running title: Mutations enabling GABA-activation of $GABA_A$ β3 homomers

To whom correspondence should be addressed: T. G. Hales: Institute of Academic Anaesthesia, Division of Systems Medicine, Ninewells Hospital, University of Dundee, Dundee, DD1 9SY, UK. Email: t.g.hales@dundee.ac.uk

Keywords: $GABA_A$ receptor, heteromeric interface, gating, GABA, propofol, patch clamp, docking

---

ABSTRACT

$GABA_A$ receptors ($GABA_A$Rs) are pentameric ligand-gated ion channels that mediate synaptic inhibition throughout the central nervous system. The $\alpha_1\beta_2\gamma_2$ receptor is the major subtype in the brain; GABA binds at the $\beta_2(+)\alpha_1(-)$ interface. The structure of the homomeric β_3 $GABA_A$R, which is not activated by GABA, has been solved. Recently, four additional heteromeric structures were reported, highlighting key residues required for agonist binding. Here, we used a protein engineering method, taking advantage of knowledge of the key binding residues, to create a $\beta_3(+)\alpha_1(-)$ heteromeric interface in the homomeric human β_3 $GABA_A$R that enables GABA-mediated activation. Substitutions were made in the complementary side of the orthosteric binding site in loop D (Y87F and Q89R), loop E (G152T) and loop G (N66D and A70T). The Q89R and G152T combination enabled low-potency activation by GABA and potentiation by propofol, but impaired direct activation by higher propofol concentrations. At higher concentrations GABA inhibited gating of β_3 $GABA_A$R variants containing Y87F, Q89R, and G152T. Reversion of Phe87 to tyrosine abolished GABA's inhibitory effect and partially recovered direct activation by propofol. This tyrosine is conserved in homomeric $GABA_A$Rs and in the *Erwinia chrysanthemi* ligand-gated ion channel and may be essential for the absence of an inhibitory effect of GABA on homomeric channels. This work demonstrated that only two substitutions, Q89R and G152T, in β_3 $GABA_A$R are sufficient to reconstitute GABA-mediated activation, and suggests that Tyr87 prevents inhibitory effects of GABA.

$GABA_A$Rs are members of the pentameric ligand-gated ion channel family and mediate fast synaptic inhibition (1). Consequently, they are important pharmacological targets (2, 3).

$GABA_A$R subunits are composed of three domains(4): 1) the extracellular domain (ECD), with ten β-strands (β1-10), one α-helix and the orthosteric binding site; 2) the transmembrane domain (TMD) comprising four helices (TM1-4), the TM2 of each subunit forms the ion pore; and 3) the intracellular domain (ICD), between TM3 and TM4, which is a site for posttranslational modification that interacts with trafficking proteins (4, 5, 6).

The orthosteric binding site is located between the α and β subunits that comprise the complementary (-) and principal (+) components, respectively. The site contains seven non-contiguous binding loops (A-G): A to C belong to the principal side, whereas loops D to G belong to the complementary side (7–9).

There are 19 different $GABA_A$R subunits that form at least 14 distinct combinations *in vivo* (10, 11), accounting for the physiological versatility and pharmacological selectivity of these channels (2). The major subtype in the central nervous system is the $\alpha_1\beta_2\gamma_2$ $GABA_A$R. The β_1, β_3 and ρ subunits can form homomers when

recombinantly expressed *in vitro*. While the homomeric β_3 has not been identified *in vivo*, it is of considerable interest as the first $GABA_AR$ to yield to high resolution structural analysis (12) and for functional studies since histaminergic ligands and propofol activate the receptor (13–16). Recently, four heteromeric $GABA_AR$ structures were published, including the major subtype (17–19). These studies determined the important residues for GABA binding and suggest that variability on the complementary subunit influences ligand selectivity (19). The homomeric β_3 cannot be activated by GABA (16, 20). This raises questions about which residues in the complementary side are required to reconstitute activation. The availability of the β_3 structure provides an opportunity to locate candidate residues.

In the present study, we investigated whether substituting amino acids in the complementary side of the β_3 $GABA_AR$ to corresponding residues in the α_1 subunit would reconstitute activation by GABA. Four β_3 mutants were designed and used for patch-clamp electrophysiology. We analysed the activation by GABA and propofol, potentiation of GABA-evoked currents by propofol and the kinetics of GABA-evoked currents. Comparative modelling and molecular docking calculations were used to predict the orientation of GABA at the orthosteric site of the mutant β_3 $GABA_AR$. Using these approaches, we demonstrated that Q89R and G152T substitutions reconstituted GABA activation of $GABA_AR$ β_3 and potentiation by propofol. In addition, we found the Y87F substitution caused GABA to inhibit receptor function.

Results

Designing the Constructs

We modified the β_3 $GABA_AR$ by replacing the ICD (residues 346 to 396) with the SQPARAA sequence to mimic the construct used to crystallize the β_3 $GABA_AR$ (12), referred to from this point as β_3-cryst (Table 1).

Docking GABA into the β_3 Orthosteric Site

Docking calculations were performed between GABA and the β_3-cryst model (Figure 1A). As far as we are aware, there are no prior reports of docking GABA into the homomeric β_3 receptor. The best GABA pose presented an energy of -38 kcal/mol, suggesting binding. Examination of residues within the orthosteric binding domain on the α_1 subunit reveal amino acids which are not shared by β_3 at key locations known to affect activation by GABA (Figure 1B). Substitution of these residues into the β_3-cryst model ($GABA_AR$ β_3 C1) improved the binding energy of GABA as evidenced by docking calculations (-46 kcal/mol). The model suggests that the GABA amino group forms a salt bridge with Glu180 on the (+) interface of the β_3 subunit (Figure 1C) and that the GABA carboxyl makes a bidentate interaction with Arg89 and a hydrogen bond with the Thr152 hydroxyl group, substituted in the (-) interface. These interactions are in agreement with the cryo-electron microscopy structures of the human $GABA_AR$ $\alpha_1\beta_2\gamma_2$ and rat $GABA_AR$ $\alpha_1\beta_1\gamma_2$ (18, 19). In addition, they were described by other studies using docking calculations with human $GABA_AR$ $\alpha_1\beta_2\gamma_2$ (21) and insect $GABA_AR$ models (21, 22).

Three substitutions reconstituted GABA activation of homomeric β_3 receptors

The Y87F, Q89R and G152T substitutions were introduced into the β_3-cryst construct, using site-directed mutagenesis. This β_3 C1 cDNA was transiently transfected into human embryonic kidney 293 cells (HEK293) for whole-cell electrophysiology recordings. Concentrations of GABA, which are maximally efficacious at heteromeric $GABA_ARs$ (1 mM) fail to activate homomeric β_3 $GABA_ARs$ (16, 20). We therefore applied higher concentrations of GABA (10 mM) to HEK293 cells expressing either β_3-cryst or β_3 C1. GABA (10 mM) evoked negligible currents mediated by β_3-cryst with current densities of 2.3 ± 0.3 pA/pF (Figure 2A). By contrast, GABA (10 mM) evoked currents mediated by β_3 C1 were larger, with current densities of 15.7 ± 4.4 pA/pF (Figure 2B). This was significantly different from β_3-cryst (n = 7, P = 0.003, *t*-test, Figure 2C). These results indicate that the amino acid substitutions (Y87F, Q89R and G152T) were sufficient to reconstitute activation by GABA.

We subsequently determined the concentration-response relationship of β_3 C1, to characterize the potency of GABA. GABA was applied at increasing concentrations to cells expressing β_3 C1. A representative example of

these currents is shown in Figure 2D. GABA-evoked current amplitudes were expressed as a percentage of the maximum and plotted as a concentration-response relationship (Figure 2E). The data indicate that GABA exhibits a biphasic concentration-response relationship, which suggests two effects: activation and inhibition. We therefore fitted a two component logistics function to the data (see Methods). GABA, up to 10 mM, activates β_3 C1, with an EC_{50} of approximately 3 mM. Higher concentrations of GABA caused a reduction in current amplitude, with an IC_{50} of approximately 50 mM. This inhibitory effect has not been observed previously in $GABA_A$Rs (9, 23–26) or in the bacterial pentameric ligand-gated ion channel, ELIC (27), which, like β_3 C1, also requires high concentrations of GABA for its activation (Supplementary Figure S1). We also observed a lack of inhibitory effect in heteromeric $GABA_A$Rs formed from β_3-cryst and β_3 C1 subunits (Supplementary Figure S2).

Kinetics of β_3 C1

In addition to the biphasic nature of the GABA concentration-response relationship, the representative currents shown in Figure 2D also display unusual kinetics. We, therefore, analysed the current activation and deactivation rates by measuring the 10-90% rise-time and by fitting a two-component exponential function, respectively (see Methods). The mean values of rise-times and weighted τ were plotted (Figure 2F and G). The individual components of the double exponential fits for deactivation can be found in Table 3. Currents evoked by lower concentrations of GABA (0.1 and 0.3 mM) were excluded from the analysis due to their small amplitudes. Consistent with the concentration-dependence of peak current activation (Figure 2E), the concentration-dependence of activation and deactivation also appears biphasic (Figure 2F and G).

GABA Does Not Cause a Voltage-Dependent Channel Block

The inhibitory effect of GABA at higher concentrations could be due to binding at a lower affinity site which blocks the channel pore. We therefore examined whether GABA causes a voltage-dependent block of β_3 C1 by comparing the current-voltage (I-V) relationships of currents evoked by 1 mM and 100 mM GABA. These concentrations were chosen because the inhibitory effect was observed at 100 mM but not at 1 mM GABA. Representative examples of the currents evoked by GABA at voltages ranging from -60 mV to 60 mV are shown in Figure 3A. GABA (1 mM) produced an outwardly rectifying I-V relationship, consistent with previous observations of currents mediated by β_3 and $\alpha_1\beta_3$ $GABA_A$Rs (16), as did 100 mM GABA. We quantified outward rectification by expressing the current amplitudes as a ratio of those evoked at -60 mV (Figure 3B). The rectification indexes calculated ($I_{60\ mV}/I_{-60\ mV}$) were 3.5 ± 0.3 and 3.6 ± 0.3 (n = 4) for 1 mM and 100 mM GABA, respectively (P = 0.8, *t*-test, n = 4). These results suggest the inhibitory effect of 100 mM GABA was not caused by voltage-dependent channel block.

Substitutions in loop G do not affect the activation of β_3 C1 by GABA

Mutagenesis studies in $GABA_AR$ $\alpha_1\beta_2\gamma_2$ indicate that the identities of α_1 loop G residues at positions 71 and 75 influence gating and, thereby, the apparent potency of GABA (9, 23, 25). In an attempt to increase the apparent potency of GABA, substitutions in loop G were made, introducing α_1 residues into β_3 C1 N66D and β_3 C1 A70T $GABA_A$Rs (residues equivalent to those at α1 positions 71 and 75, respectively). Neither the potency nor the efficacy of GABA was affected (one-way ANOVA *post hoc* Dunnett's, P = 0.8, $F_{(2,12)}$ = 0.28). This is perhaps not surprising due to the conservative nature of the N66D and A40T substitutions (Supplementary Figure S3 and Supplementary Table S1).

A Loop D Tyr Conserved in Homomeric Receptors Prevents Block by GABA

An amino acid sequence alignment of the pentameric ligand-gated ion channel subunits that form homomeric GABA-activated receptors, including ELIC, reveals conservation of the Tyr at the position equivalent to β_3 amino acid 87 (Supplementary Figure S4A). We investigated whether replacement of ELIC Tyr38 with Phe affects activation by GABA. Interestingly, GABA failed to evoke currents mediated by ELIC Y38F, despite the conservative nature of this substitution (Supplementary Figure S4C). These data suggest that the Phe is detrimental to ELIC function. Since ELIC, $GABA_A$ ρ, and $GABA_A$ β all contain a Tyr,

this residue may be necessary for preventing block of homomeric receptors by GABA. We tested the hypothesis that the Tyr is required in β_3 receptors to prevent inhibitory effects of GABA at high concentrations by creating the β_3 C1 F87Y, in which the Phe87 was reverted back to the tyrosine found in WT β_3.

Cells expressing β_3 C1 F87Y were voltage-clamped at -60 mV and GABA-evoked currents were recorded. Representative examples are shown in Figure 4A. The current amplitudes were expressed as a percentage of maximum and plotted as a concentration-response relationship, which was fitted with a single component logistic function (Figure 4B). The potency of activation by GABA was similar, when compared to β_3 C1 (P = 0.2, n = 4, *t*-test; Table 2), as was the maximum current density (P = 0.6, n = 4, *t*-test; Table 2). However, the inhibition by 100 mM GABA was absent in β_3 C1 F87Y, with a significant difference in the current amplitude evoked by 100 mM GABA compared to that mediated by β_3 C1 (P = 0.003, n = 4, *t*-test). Similarly, higher concentrations of GABA (300 mM) did not reduce GABA-mediated current amplitude (Supplementary Figure S5), indicating that the inhibitory component was abolished with the F87Y substitution. Furthermore, the rate of activation of β_3 C1 F87Y increased with GABA concentration and was not biphasic (Figure 4C). There was also no apparent influence of GABA concentration on deactivation (Figure 4D), consistent with the previous data for $GABA_A$Rs (29) and ELIC (Supplementary Figure S1C and D).

Effects of Propofol on β_3 Mutants

Consistent with a previous report of β_3 receptor activation (16), propofol (30 μM) evoked inward currents when applied locally to HEK293 cells expressing β_3-cryst recorded under voltage-clamp at -60 mV (Figure 5A); however, no response was observed in cells expressing β_3 C1 (Figure 5B). A partial recovery of propofol direct activation was observed in β_3 C1 F87Y (Figure 5C), as evidenced by the significant difference in current densities between β_3-cryst and β_3 C1 (n = 10, *t*-test, $P < 0.0001$) and between β_3 C1 and β_3 C1 F87Y (n = 10, *t*-test, P = 0.007; Figure 5D).

Potentiation, activation and blockade of $GABA_A$Rs occur at different propofol concentrations, consistent with the possibility of distinct sites with differing affinities (30–32). The substitutions introduced in β_3 C1 and β_3 C1 F87Y may have affected the gating mechanism or induced structural rearrangements that disrupt the binding site of propofol responsible for the direct activation of the receptor.

We investigated whether propofol can potentiate GABA-induced currents mediated by β_3 C1 and β_3 C1 F87Y. Cells were stepped from GABA (1 mM) to a solution of GABA (1 mM) plus propofol (10 or 30 μM), and back to GABA (1 mM). This concentration of GABA corresponds to EC_{25} according to the concentration-response relationship, allowing ample scope for enhancement (Figure 2E).

As previously observed (Figure 2A), GABA failed to evoke currents when applied to cells expressing β_3-cryst (Figure 6A). The current observed when GABA was applied with propofol (30 μM) to cells expressing β_3-cryst was equivalent to that observed when propofol was applied alone (Figure 5), indicating a lack of interaction with GABA (Figure 6A). By contrast, in cells expressing $GABA_A$R β_3 C1, propofol (10 and 30 μM) enhanced GABA-evoked currents (Figure 6B and C) by 404 ± 106% (n = 3) and 405 ± 67% (n = 7), respectively (Figure 6F). When applied alone, propofol did not evoke a current. Therefore, the enhancement by propofol of GABA-evoked currents mediated by β_3 C1 is caused by potentiation rather than additive activation. Propofol (10 and 30 μM) also enhanced GABA-induced currents mediated by β_3 C1 F87Y (Figure 6D and E) by 242 ± 62% (n = 5) and 663 ± 82% (n = 8), respectively (Figure 6F). The significant increase (one-way ANOVA *post hoc* Tukey's, P = 0.008, F (3,19) = 5.3) in current enhancement by propofol (30 μM) is due in this case to the additive effect of direct activation, rather than increased potentiation. However, the observation that propofol (10 μM) alone failed to activate a current in the absence of GABA, indicates that similar to $GABA_A$R β_3 C1, β_3 C1 F87Y also support propofol-evoked potentiation.

Discussion

This study demonstrates that the replacement of two key residues in the orthosteric binding site of the β_3 subunit (Gln89 and Gly152), by the equivalent ECD loci in the α subunit, Arg

and Thr, respectively, enables gating of β_3 receptors by GABA. Docking to the β_3 C1 model, which includes these substitutions plus the additional F87Y substitution, confirmed the interaction of GABA with all three of these binding residues. The favored GABA binding pose was similar to that of heteromeric $GABA_AR$ structures (18, 19), observations in previous docking studies using the mammalian heteromeric and the insect homomeric $GABA_A$Rs (21, 22) and in general agreement with the literature (21, 33, 34). The GABA carboxyl makes a bidentate interaction with Arg89 and a hydrogen bond with the Thr152 hydroxyl group in β_3 C1. The same interactions were reported in heteromeric $GABA_AR$ structures solved in the presence of the agonist (18, 19). In addition, site-directed mutagenesis studies demonstrate that substitution of these residues in the α subunit affects GABA potency in $GABA_AR$ $\alpha_1\beta_2\gamma_2$ and $GABA_AR$ $\alpha_1\beta_2$ (24, 35, 36).

Taken together the results of docking and functional analysis are consistent with the idea that the introduction of Q89R and G152T substitutions into β_3 generates a heteromeric $\beta_3(+)\alpha_1(-)$-like interface capable of activation by GABA albeit at high concentrations (> 300 μM).

GABA concentrations above 10 mM caused a blocking effect in β_3 C1. This has not been observed in other physiologically relevant heteromeric $GABA_A$Rs (9, 23–26) or in ELIC (27). The effect was abolished when the phenylalanine in β_3 C1 was reverted back to tyrosine: F87Y. Interestingly, this effect was also abolished in heteromeric $GABA_A$Rs formed from β_3 C1 (where position 87 is a Phe) and β_3-cryst subunits (where position 87 is a Tyr). The apparent potency of GABA-mediated activation is not altered in these heteromeric $GABA_A$Rs. While the stoichiometry of heteromeric $GABA_A$Rs formed from β3 C1 and β3-cryst subunits are not known, our data suggest that the incorporation of one or more Tyr87 is sufficient to prevent GABA-mediated blockade while preserving GABA-mediated activation, highlighting the importance of this residue in $GABA_AR$ function.

The kinetics of GABA-evoked currents mediated by β_3 C1 $GABA_A$Rs were also unusual. Activation and deactivation became slower and then faster with increasing concentrations of GABA, while the kinetics in β_3 C1 F87Y $GABA_A$Rs were more consistent with those of heteromeric $GABA_A$Rs (29) and ELIC (Supplementary Figure S1). Interestingly, activation and deactivation rates of GABA-evoked currents mediated by β_3 C1 $GABA_A$Rs appear similar to those described for $GABA_A$Rs activated in the presence of modulators, such as propofol (37) and benzodiazepines (38). In addition to its role as an agonist and an inhibitor of β_3 C1 $GABA_A$Rs, GABA may also act as a positive allosteric modulator. In the homomeric β_3 C1 $GABA_A$Rs, GABA may bind to all five subunit interfaces and the Hill slope of 1.3 suggests cooperativity between at least two of these sites. It is possible that binding to additional orthosteric sites may result in potentiation, similar to the effect of benzodiazepines (38). However, our data with β_3 C1 and β_3-cryst heteromeric $GABA_A$Rs suggest that GABA-mediated activation does not require GABA binding to all interfaces.

Moreover, bell-shaped concentration-response curves have been described for allosteric activators and modulators of $GABA_A$Rs, such as propofol (16), valerenic acid (39) and pentobarbital (40–42). Pentobarbital, at low concentrations (low micromolar), can potentiate $GABA_AR$ currents by increasing the mean open duration. Higher concentrations (high micromolar) of pentobarbital can activate $GABA_A$Rs, and millimolar concentrations can inhibit the channel, slowing deactivation (42). Similarly, GABA may act as an agonist, modulator and inhibitor of β_3 C1. However, the inhibition is not through a voltage-dependent channel block. Instead there may be a lower affinity inhibitory site for GABA. A similar mechanism has been proposed for the inhibitory effect observed with high concentrations of propofol (32).

While the potentiation of GABA-evoked currents was unaffected, propofol's direct activation of β_3 C1 was impaired compared to β_3-cryst. There was partial recovery of propofol activated current medicated by β_3 C1 F87Y $GABA_A$Rs. It is clear that substitutions in the orthosteric site can influence direct activation by propofol despite its binding site being in the TM region. In keeping with a need for conformational rearrangement in the orthosteric binding site during gating by propofol, the activation is also inhibited by bicuculline (43). Furthermore, we recently demonstrated faster deactivation of

propofol-evoked currents with α_1 loop D (F64C) and loop G (T47R) substitutions in $GABA_AR$ $\alpha_1\beta_2\gamma_2$, which adds additional support for a role of residues in or near the orthosteric binding site in the efficacy of gating by an allosteric agonist (26). Several studies suggest that gating by both orthosteric and allosteric agonists involves an interaction of the loops in the ECD with the TMD, particularly the loops between the β1-β2 strands and TM2-TM3 helices (44–47) and between β6-β7 strands and TM2-TM3 helices (12). It is important to note that loop G is located in β1 strand, loop D in β2, and loop E in β6. The substitutions in $GABA_AR$ β_3 C1 are located in loops D and E; therefore, they may affect a concerted gating mechanism.

It is not yet clear why the substitution Y87F causes GABA to act as an inhibitor of β_3 C1 $GABA_ARs$ at high concentrations and impair propofol direct activation. The substitution may affect channel gating, consistent with previous mutagenesis studies of homologous residues in $GABA_AR$ ρ_1 that produced spontaneous opening and affected GABA, trans-4-aminocrotonic acid and imidazole-4-acetic acid potencies (48) and in $GABA_AR$ $\alpha_1\beta_{1,2}\gamma_2$ that affected GABA potency and kinetics (9, 49).

The tyrosine is found in all $GABA_AR$ β and ρ subunits and in ELIC. The latter two form homomers that can be activated by GABA (20, 27, 50). Tyrosine may prevent an inhibitory effect of GABA in homomeric receptors, its substitution to phenylalanine may enable GABA to bind at another lower affinity site and inhibit gating.

In summary, this study demonstrated that only two substitutions (Q89R and G152T) were required to reconstitute activation by GABA in homomeric β_3 constructs. The potency of GABA was two orders of magnitude lower compared to heteromeric $GABA_ARs$. Similar to heteromeric $GABA_ARs$, propofol potentiated submaximal GABA-evoked currents and caused direct activation of β_3 C1 F87Y receptors. Surprisingly, the conservative replacement of Tyr87 by phenylalanine abolished gating by propofol and caused GABA to have inhibitory effects at high concentrations.

These findings identify structural requirements for the reconstitution of a functional GABA binding site in β_3 homomeric receptors by transplanting key residues of the α subunit at the heteromeric interface. This approach provides a novel method for developing a better understanding of the structural requirements for gating.

Experimental procedures

Constructs

The $GABA_AR$ constructs were designed based on the published $GABA_AR$ β_3 structure, *i.e.*, substituting the ICD for the amino acid sequence SQPARAA (12) and using the human $GABA_AR$ β_3 sequence (UniProt: P28472). The ELIC WT construct (UniProt: P0C7B7) was modified for expression in HEK293 cells, adding a Kozak sequence before the cDNA and using the human 5-HT3A subunit signal peptide as previously described (51).

Mutagenesis of $GABA_AR$ β_3 Subunit

Genes encoding the human $GABA_AR$ β_3 WT, human $GABA_AR$ β_3 C1 and *E. chrysanthemi* ELIC WT were ordered from GeneWiz and cloned into pRK5 and pcDNA3.1 vectors. Single point mutations were performed by overlap extension PCR (52). QuikChange® tool (Agilent) was utilized to design the primers. Multiple template-based sequential PCRs were used to obtain the 5-HT3A signal peptide-ELIC WT chimera (53).

PCR products, mutagenesis reactions and ligations were verified using agarose gel electrophoresis and DNA sequencing (DNA Sequencing and Services, University of Dundee). The PCR and cloning reagents were bought from Agilent and Thermo Fisher, respectively.

The genes cloned into their respective vectors were used to transform *E. coli* DH5α cells and grow cultures (500 mL of lysogeny broth media with 50 μg/mL carbenicillin) at 37°C overnight. The cells were harvested (6000 g, 4°C, 20 min) and used for Maxiprep (Qiagen) to obtain a higher yield of the plasmid.

Cell Culture and Transfection

HEK-293 cells were maintained in Dulbecco's modified Eagle's medium (DMEM) supplemented with 10% fetal bovine serum, 100 μg/mL penicillin and 100 units/mL streptomycin at 37ºC and 5% CO_2. Cells were seeded at low density in 35 mm dishes for electrophysiology. Transfections were performed by calcium phosphate precipitation, using 1 μg of total cDNA per dish, as described previously (26). The cDNAs encoding $GABA_AR$ β_3 WT and the mutants were

in the pRK5 mammalian expression vector. The cDNA encoding ELIC WT was cloned into the pcDNA3.1 vector. The cDNA that encodes enhanced green fluorescence protein (0.1 μg, in pEGFP vector) was included to identify successfully transfected cells using fluorescence microscopy. Cells were washed with media 16 h after transfection and used for voltage-clamp electrophysiology after 48-72 h. The tissue culture reagents were obtained from Invitrogen.

Electrophysiology

The whole-cell configuration of the patch clamp technique was used to record propofol- or GABA-evoked currents from HEK-293 cells transiently expressing $GABA_AR$ β_3 WT, $GABA_AR$ β_3 mutants and ELIC WT. Recording electrodes were fabricated from borosilicate glass capillaries with resistances of 1.2-3.5 MΩ when filled with intracellular solution, which contained (in mM): 140 CsCl, 2 $MgCl_2$, 1.1 EGTA, 3 Mg-ATP and 10 HEPES (pH 7.4 with CsOH). The extracellular solution contained (in mM): 140 NaCl, 4.7 KCl, 1.2 $MgCl_2$, 2.5 $CaCl_2$, 10 HEPES and 10 glucose (pH 7.4 with NaOH). The solutions for ELIC WT were different. The intracellular solution contained (in mM): 140 NaCl, 0.5 $CaCl_2$, 5 EGTA and 10 HEPES (pH 7.4 with NaOH). The extracellular solution contained (in mM): 140 NaCl, 4.7 KCl, 1.2 $MgCl_2$, 0.2 $CaCl_2$, 10 HEPES and 10 glucose (pH 7.4 with NaOH).

Cells were voltage-clamped at an electrode potential of -60 mV, unless otherwise stated. Currents were evoked by rapid application of GABA or propofol using the three-pipe Perfusion Fast Step system (Warner Instruments), as described previously (26).

The data were recorded using an Axopatch 200B amplifier (Axon Instruments), low pass filtered at 2 kHz, digitized at 10 kHz using a Digidata 1320 A interface (Molecular Devices) and acquired using pCLAMP8 software (Molecular Devices).

Data Analyses

The analyses were carried out using Clampfit 10 (Molecular Devices), Excel 2011 (Microsoft) and Prism 5 (GraphPad). Peak amplitudes were measured using averaged traces from at least three currents. GABA-evoked current amplitudes were expressed as a percentage of the maximum and plotted as a concentration-response relationship. The following logistics and bell-shaped equations were fitted to the data points to determine the Hill slopes (n^H) and the EC_{50}.

Logistic:

$$f([GABA]) = \frac{Minimum + (Maximum - Minimum)}{1 + 10^{(logEC_{50} - [GABA]) \times n^H}}$$

Bell-shaped:

$$Activation = \frac{Maximum - (Maximum + Minimum/2)}{1 + 10^{(logEC_{50} - [GABA]) \times n^{H\,1}}}$$

$$Inhibition = \frac{Minimum - (Maximum + Minimum/2)}{1 + 10^{([GABA] - logEC_{50}) \times n^{H\,2}}}$$

Peak current densities were calculated by normalising the peak current amplitude to the cell capacitance. The potentiation effect of propofol was calculated using the formula:

$$\%\ potentiation = \frac{(I_{pot} - I_{GABA})}{I_{GABA}} \times\ 100$$

where I_{pot} and I_{GABA} represent the potentiated and control peak current amplitudes, respectively. Activation rates were measured using 10-90% rise time of the GABA-evoked current. Deactivation rate was calculated by fitting a double-exponential function to the decay phase of the GABA-evoked current:

$$f(t) = A_1 e^{-t/\tau_1} + A_2 e^{-t/\tau_2}$$

where τ_N are time constants and A_N represent the proportion of the particular τ. The best-fit number of exponential terms was determined using an F-test with confidence at the 95% level. Deactivation rates were provided as weighted τ values, using:

$$weighted\ \tau = A_1 \times \tau_1 + A_2 \times \tau_2$$

Statistical Analyses

Data are presented as mean ± SD. Difference of three or more groups were compared using one-way ANOVA. Subsequent multiple pairwise comparisons were performed using the Dunnett's or Tukey's correction. The Student's *t*-test was used for other pairwise comparisons. In

all cases $P < 0.05$ was considered statistically significant. Statistical analyses were performed on Prism 5 (GraphPad).

Comparative Modelling

The model for $GABA_AR$ β_3 C1 was generated in Modeller v9.13 (54) using the $GABA_AR$ β_3 structure (PDBID: 4COF) (12) as a template. The proteins share 99% of sequence identity according to MUSCLE sequence alignment (55), being suitable for comparative modelling. The best model according to energy, spatial restraints and stereochemistry was chosen using the Discrete Optimized Protein Energy (DOPE) score (56) and Ramachandran plot (57).

Molecular Docking

Molsoft ICM v.3.8-3 (58) was used to perform docking calculations of GABA into the $GABA_AR$ β_3 WT structure (PDBID: 4COF) and the $GABA_AR$ β_3 C1 model. The preparation of the receptor and ligand models involved adding hydrogens, calculating charges at pH 7.0, deleting waters, treating the receptor as rigid and the ligand flexible. The whole receptor or potentially important residues of the binding site was selected (principal side: D95-L99, L152-T161 and N197-R207; complementary side: N41-A45, M61-Y66, N113-L118, L125-A135 and A174-V178) and a box was created around the selection with a 3-Å distance between the residues and the edges. The results were ranked according to the ICM score, which takes into consideration the quality of the complex based on van der Waals interactions and the internal force field energy of the ligand (58).

Acknowledgments:
CGC thanks Capes Science without Borders scheme (BEX 0321/13-3) for funding.

Conflict of interest: The authors declare that they have no conflicts of interest with the contents of this article.

References

1. Sigel, E., and Steinmann, M. E. (2012) Structure, function, and modulation of GABAA receptors. *J. Biol. Chem.* **287**, 40224–40231
2. Johnston, G. A. R. (2005) GABA(A) receptor channel pharmacology. *Curr. Pharm. Des.* **11**, 1867–1885
3. Zhang, J., Xue, F., Liu, Y., Yang, H., and Wang, X. (2013) The structural mechanism of the cys-loop receptor desensitization. *Mol. Neurobiol.* **48**, 97–108
4. Unwin, N. (2005) Refined structure of the nicotinic acetylcholine receptor at 4 Å resolution. *J. Mol. Biol.* **346**, 967–989
5. Kelley, S. P., Dunlop, J. I., Kirkness, E. F., Lambert, J. J., and Peters, J. A. (2003) A cytoplasmic region determines single-channel conductance in 5-HT3receptors. *Nature*. **424**, 321–324
6. Baptista-Hon, D. T., Deeb, T. Z., Lambert, J. J., Peters, J. A., and Hales, T. G. (2013) The minimum M3-M4 loop length of neurotransmitteractivated pentameric receptors is critical for the structural integrity of cytoplasmic portals. *J. Biol. Chem.* **288**, 21558–21568
7. Nys, M., Kesters, D., and Ulens, C. (2013) Structural insights into Cys-loop receptor function and ligand recognition. *Biochem. Pharmacol.* **86**, 1042–1053
8. Hibbs, R. E., and Gouaux, E. (2011) Principles of activation and permeation in an anion-selective Cys-loop receptor. *Nature*. **474**, 54–60
9. Baptista-Hon, D. T., Krah, A., Zachariae, U., and Hales, T. G. (2016) A role for loop G in the β1 strand in GABAA receptor activation. *J. Physiol.* **594**, 5555–5571
10. Whiting, P. J. (2003) GABA-A receptor subtypes in the brain: A paradigm for CNS drug discovery? *Drug Discov. Today*. **8**, 445–450
11. Dawson, G. R., Collinson, N., and Atack, J. R. (2005) Development of subtype selective GABAAmodulators. *CNS Spectr.* **10**, 21–27
12. Miller, P. S., and Aricescu, A. R. (2014) Crystal structure of a human GABAA receptor. *Nature*. **512**, 270–275

13. Saras, A., Gisselmann, G., Vogt-Eisele, A. K., Erlkamp, K. S., Kletke, O., Pusch, H., and Hatt, H. (2008) Histamine action on vertebrate GABAA receptors: Direct channel gating and potentiation of GABA responses. *J. Biol. Chem.* **283**, 10470–10475
14. Seeger, C., Christopeit, T., Fuchs, K., Grote, K., Sieghart, W., and Danielson, U. H. (2012) Histaminergic pharmacology of homo-oligomeric β3 γ-aminobutyric acid type A receptors characterized by surface plasmon resonance biosensor technology. *Biochem. Pharmacol.* **84**, 341–351
15. Kumar, M., and Dillon, G. H. (2016) Assessment of direct gating and allosteric modulatory effects of meprobamate in recombinant GABAA receptors. *Eur. J. Pharmacol.* **775**, 149–158
16. Davies, P. A., Kirkness, E. F., and Hales, T. G. (1997) Modulation by general anaesthetics of rat GABA(A) receptors comprised of α1β3 and β3 subunits expressed in human embryonic kidney 293 cells. *Br. J. Pharmacol.* **120**, 899–909
17. Miller, P., Masiulis, S., Malinauskas, T., Kotecha, A., Rao, S., Chavali, S., Colibus, L. De, Pardon, E., Hannan, S., Scott, S., Sun, Z., Frenz, B., Klesse, G., Li, S., Diprose, J., Siebert, A., Esnouf, R., DiMaio, F., Tucker, S., Smart, T., Steyaert, J., Babu, M., Sansom, M., Huiskonen, J., and Aricescu, R. (2018) Heteromeric GABAA receptor structures in positively-modulated active states. *bioRxiv*. 10.1101/338343
18. Phulera, S., Zhu, H., Yu, J., Claxton, D. P., Yoder, N., Yoshioka, C., and Gouaux, E. (2018) Cryo-EM structure of the benzodiazepine-sensitive α1β1γ2S tri-heteromeric GABAA receptor in complex with GABA. *Elife*. **7**, 163–170
19. Zhu, S., Noviello, C. M., Teng, J., Walsh, R. M., Kim, J. J., and Hibbs, R. E. (2018) Structure of a human synaptic GABAA receptor. *Nature*. **559**, 67–72
20. Wooltorton, J. R., Moss, S. J., and Smart, T. G. (1997) Pharmacological and physiological characterization of murine homomeric β3 GABAA receptors. *Eur. J. Neurosci.* **9**, 2225–2235
21. Bergmann, R., Kongsbak, K., Sørensen, P. L., Sander, T., and Balle, T. (2013) A Unified Model of the GABAA Receptor Comprising Agonist and Benzodiazepine Binding Sites. *PLoS One*. **8**, e52323
22. Ashby, J. A., McGonigle, I. V., Price, K. L., Cohen, N., Comitani, F., Dougherty, D. A., Molteni, C., and Lummis, S. C. R. (2012) GABA binding to an insect GABA receptor: A Molecular Dynamics and Mutagenesis Study. *Biophys. J.* **103**, 2071–2081
23. Jones, M. V, Sahara, Y., Dzubay, J. a, and Westbrook, G. L. (1998) Defining affinity with the GABAA receptor. *J. Neurosci.* **18**, 8590–8604
24. Kloda, J. H., and Czajkowski, C. (2007) Agonist-, antagonist-, and benzodiazepine-induced structural changes in the α1 Met113-Leu132 region of the GABAA receptor. *Mol. Pharmacol.* **71**, 483–93
25. Hollands, E. C., Dale, T. I. M. J., Baxter, A. W., Meadows, H. J., Powell, A. J., Clare, J. J., Trezise, D. J., Derek, J., and Cells, H.- (2009) Population patch-clamp electrophysiology analysis of recombinant GABAA α1β3γ2 channels expressed in HEK-293 cells. *J. Biomol. Screen.* **14**, 769–80
26. Baptista-Hon, D. T., Gulbinaite, S., and Hales, T. G. (2017) Loop G in the GABAA receptor α1 subunit influences gating efficacy. *J. Physiol.* **595**, 1725–1741
27. Spurny, R., Ramerstorfer, J., Price, K., Brams, M., Ernst, M., Nury, H., Verheij, M., Legrand, P., Bertrand, D., Bertrand, S., Dougherty, D. A., de Esch, I. J. P., Corringer, P.-J., Sieghart, W., Lummis, S. C. R., and Ulens, C. (2012) Pentameric ligand-gated ion channel ELIC is activated by GABA and modulated by benzodiazepines. *Proc. Natl. Acad. Sci.* **109**, E3028–E3034
28. Colquhoun, D. (1998) Binding, gating, affinity and efficacy: The interpretation of structure-activity relationships for agonists acid of the effects of mutating receptors. *Br. J. Pharmacol.* **125**, 923–947
29. Lavoie, A. M., Tingey, J. J., Harrison, N. L., Pritchett, D. B., and Twyman, R. E. (1997) Activation and deactivation rates of recombinant GABA(A) receptor channels are dependent on α-subunit isoform. *Biophys. J.* **73**, 2518–2526

30. Hales, T. G., and Lambert, J. J. (1991) The actions of propofol on inhibitory amino acid receptors of bovine adrenomedullary chromaffin cells and rodent central neurones. *Br. J. Pharmacol.* **104**, 619–628
31. Orser, B. A., Wang, L. Y., Pennefather, P. S., and MacDonald, J. F. (1994) Propofol Modulates Activation and Desensitization of GABA(A) Receptors in Cultured Murine Hippocampal-Neurons. *J. Neurosci.* **14**, 7747–7760
32. Adodra, S., and Hales, T. G. (1995) Potentiation, activation and blockade of GABAA receptors of clonal murine hypothalamic GT1- 7 neurones by propofol. *Br. J. Pharmacol.* **115**, 953–960
33. Defeudis, F. V. (1986) Muscimol and Central Nervous System γ-Aminobutyric Acid Receptors: Studies with Ligand-Binding Techniques. in *The Receptors*, pp. 135–152, Academic Press
34. Rognan, D., Boulanger, T., Hoffmann, R., Vercauteren, D. P., Andre, J. M., Durant, F., and Wermuth, C. G. (1992) Structure and molecular modeling of GABAA receptor antagonists. *J. Med. Chem.* **35**, 1969–77
35. Boileau, A. J., Glen Newell, J., and Czajkowski, C. (2002) GABAA receptor β2 Tyr97 and Leu99 line the GABA-binding site. Insights into mechanisms of agonist and antagonist actions. *J. Biol. Chem.* **277**, 2931–2937
36. Holden, J. H., and Czajkowski, C. (2002) Different residues in the GABAA receptor α1T60-α1K70 region mediate GABA and SR-95531 actions. *J. Biol. Chem.* **277**, 18785–18792
37. Bai, D., Pennefather, P. S., MacDonald, J. F., and Orser, B. a (1999) The general anesthetic propofol slows deactivation and desensitization of GABA(A) receptors. *J. Neurosci.* **19**, 10635–10646
38. Mellor, J. R., and Randall, A. D. (1997) Frequency-dependent actions of benzodiazepines on GABAA receptors in cultured murine cerebellar granule cells. *J. Physiol.* **503 (Pt 2**, 353–69
39. Khom, S., Baburin, I., Timin, E., Hohaus, A., Trauner, G., Kopp, B., and Hering, S. (2007) Valerenic acid potentiates and inhibits GABAA receptors: Molecular mechanism and subunit specificity. *Neuropharmacology*. **53**, 178–187
40. Schwartz, R. D., Suzdak, P. D., and Paul, S. M. (1986) gamma-Aminobutyric acid (GABA)- and barbiturate-mediated 36Cl- uptake in rat brain synaptoneurosomes: evidence for rapid desensitization of the GABA receptor-coupled chloride ion channel. *Mol Pharmacol*. **30**, 419–426
41. Thompson, S. A., Whiting, P. J., and Wafford, K. A. (1996) Barbiturate interactions at the human GABAA receptor: dependence on receptor subunit combination. *Br. J. Pharmacol.* **117**, 521–527
42. Feng, H., Bianchi, M., and Macdonald, R. (2004) Pentobarbital differentially modulates α1β3δ and α1β3γ2L GABAA receptor currents. *Mol. Pharmacol.* **66**, 988–1003
43. McCartney, M. R., Deeb, T. Z., Henderson, T. N., and Hales, T. G. (2007) Tonically active GABAA receptors in hippocampal pyramidal neurons exhibit constitutive GABA-independent gating. *Mol. Pharmacol.* **71**, 539–548
44. Kash, T. L., Jenkins, A., Kelley, J. C., Trudell, J. R., and Harrison, N. L. (2003) Coupling of agonist binding to channel gating in the GABAA receptor. *Nature*. **421**, 272–275
45. Hales, T. G., Deeb, T. Z., Tang, H., Bollan, K. a, King, D. P., Johnson, S. J., and Connolly, C. N. (2006) An asymmetric contribution to gamma-aminobutyric type A receptor function of a conserved lysine within TM2-3 of α1, β2, and γ2 subunits. *J. Biol. Chem.* **281**, 17034–43
46. Calimet, N., Simoes, M., Changeux, J.-P., Karplus, M., Taly, A., and Cecchini, M. (2013) A gating mechanism of pentameric ligand-gated ion channels. *Proc. Natl. Acad. Sci. U. S. A.* **110**, E3987-96
47. Althoff, T., Hibbs, R. E., Banerjee, S., and Gouaux, E. (2014) X-ray structures of GluCl in apo states reveal a gating mechanism of Cys-loop receptors. *Nature*. **512**, 333–337
48. Torres, V. I., and Weiss, D. S. (2002) Identification of a tyrosine in the agonist binding site of the homomeric ρ1 γ-aminobutyric acid (GABA) receptor that, when mutated, produces spontaneous opening. *J. Biol. Chem.* **277**, 43741–43748
49. Szczot, M., Kisiel, M., Czyzewska, M. M., and Mozrzymas, J. W. (2014) α1F64 Residue at GABA(A) receptor binding site is involved in gating by influencing the receptor flipping

transitions. *J. Neurosci.* **34**, 3193–3209
50. Harrison, N. J., and Lummis, S. C. R. (2006) Locating the carboxylate group of GABA in the homomeric rho GABAAreceptor ligand-binding pocket. *J. Biol. Chem.* **281**, 24455–24461
51. Trumper, P., Hunter, W. N., and Hales, T. G. (2014) *Development of a high throughput ligand screening method and structural studies of pentameric ligand gated ion channels*. Ph.D. thesis, University of Dundee
52. Heckman, K. L., and Pease, L. R. (2007) Gene splicing and mutagenesis by PCR-driven overlap extension. *Nat. Protoc.* **2**, 924–932
53. Shan, Q., and Lynch, J. W. (2010) Chimera construction using multiple-template-based sequential PCRs. *J. Neurosci. Methods*. **193**, 86–89
54. Webb, B., and Sali, A. (2014) Comparative protein structure modeling using MODELLER. *Curr. Protoc. Bioinforma.* **2014**, 5.6.1-5.6.32
55. Edgar, R. C. (2004) MUSCLE: Multiple sequence alignment with high accuracy and high throughput. *Nucleic Acids Res.* **32**, 1792–1797
56. Shen, M., and Sali, A. (2006) Statistical potential for assessment and prediction of protein structures. *Protein Sci.* **15**, 2507–2524
57. Laskowski, R. A., MacArthur, M. W., Moss, D. S., and Thornton, J. M. (1993) PROCHECK: a program to check the stereochemical quality of protein structures. *J. Appl. Crystallogr.* **26**, 283–291
58. Neves, M. A. C., Totrov, M., and Abagyan, R. (2012) Docking and scoring with ICM: The benchmarking results and strategies for improvement. *J. Comput. Aided. Mol. Des.* **26**, 675–686

FOOTNOTES

The abbreviations used are: ECD, extracellular domain; ELIC, *Erwinia chrysanthemi* ligand-gated ion channel; $GABA_A$Rs, GABA type A receptors; HEK293, human embryonic kidney cells 293; ICD, intracellular domain; TMD, transmembrane domain.

Table 1. Protein constructs.

Construct Name	ECD Interface	Substitutions
$GABA_AR$ β_3-cryst	$\beta_3(+)\beta_3(-)$	Substitute ICD (346-396) for SQPARAA
$GABA_AR$ β_3 C1	$\beta_3(+)\alpha_1$	β_3-cryst + Y87F, Q89R, G152T
$GABA_AR$ β_3 C1 N66D	$\beta_3(+)\alpha_1$	C1 + N66D
$GABA_AR$ β_3 C1 A70T	$\beta_3(+)\alpha_1$	C1 + A70T
$GABA_AR$ β_3 C1 F87Y	$\beta_3(+)\alpha_1$	β_3-cryst + Q89R, G152T

Table 2. Summary of Hill slope, EC_{50} and current density values obtained for GABA activation of $GABA_AR$ β_3 C1 and F87Y. Mean ± SD Hill slope and EC_{50} values obtained from logistic function fit parameters of individual experiments. Mean ± SD current densities evoked by peak concentrations of GABA. No significant differences between $GABA_AR$ β_3 C1 and F87Y were observed (*t*-test; EC_{50} P = 0.2; current densities P = 0.6). n = number of experiments.

Receptor	Hill slope	EC_{50} (mM)	Current density (pA/pF)	n
$GABA_AR$ β_3 C1	1.3 ± 0.4	2.9 ± 2.1	-15.7 ± 12.5	4
$GABA_AR$ β_3 C1 F87Y	1.2 ± 0.3	1.3 ± 0.6	-17.1 ± 11.9	4

Table 3. Mean ± SD of the deactivation components in $GABA_AR$ β_3 C1 and F87Y. No significant differences were observed between the mutants (n = 4, P = 0.1052, F (9,34) = 1.8, one-way ANOVA *post hoc* Tukey's).

	[GABA] (mM)	τ_f	$\%_f$	τ_s	$\%_s$	Weighted τ
β_3 C1	1	34 ± 3	59 ± 5	253 ± 3	41 ± 5	142 ± 54
	3	56 ± 32	48 ± 14	347 ± 139	52 ± 14	181 ± 97
	10	58 ± 45	47 ± 2	342 ± 137	72 ± 26	243 ± 130
	30	39 ± 10	37 ± 10	282 ± 98	72 ± 20	260 ± 124
	100	37 ± 23	63 ± 33	261 ± 125	37 ± 33	84 ± 29
β_3 C1 F87Y	1	40 ± 9	64 ± 13	424 ± 142	36 ± 13	176 ± 56
	3	51 ± 19	66 ± 11	345 ± 139	34 ± 11	151 ± 76
	10	67 ± 30	56 ± 13	337 ± 79	44 ± 14	194 ± 66
	30	79 ± 49	52 ± 15	511 ± 173	48 ± 15	287 ± 114
	100	63 ± 7	77 ± 17	518 ± 232	23 ± 17	198 ± 171

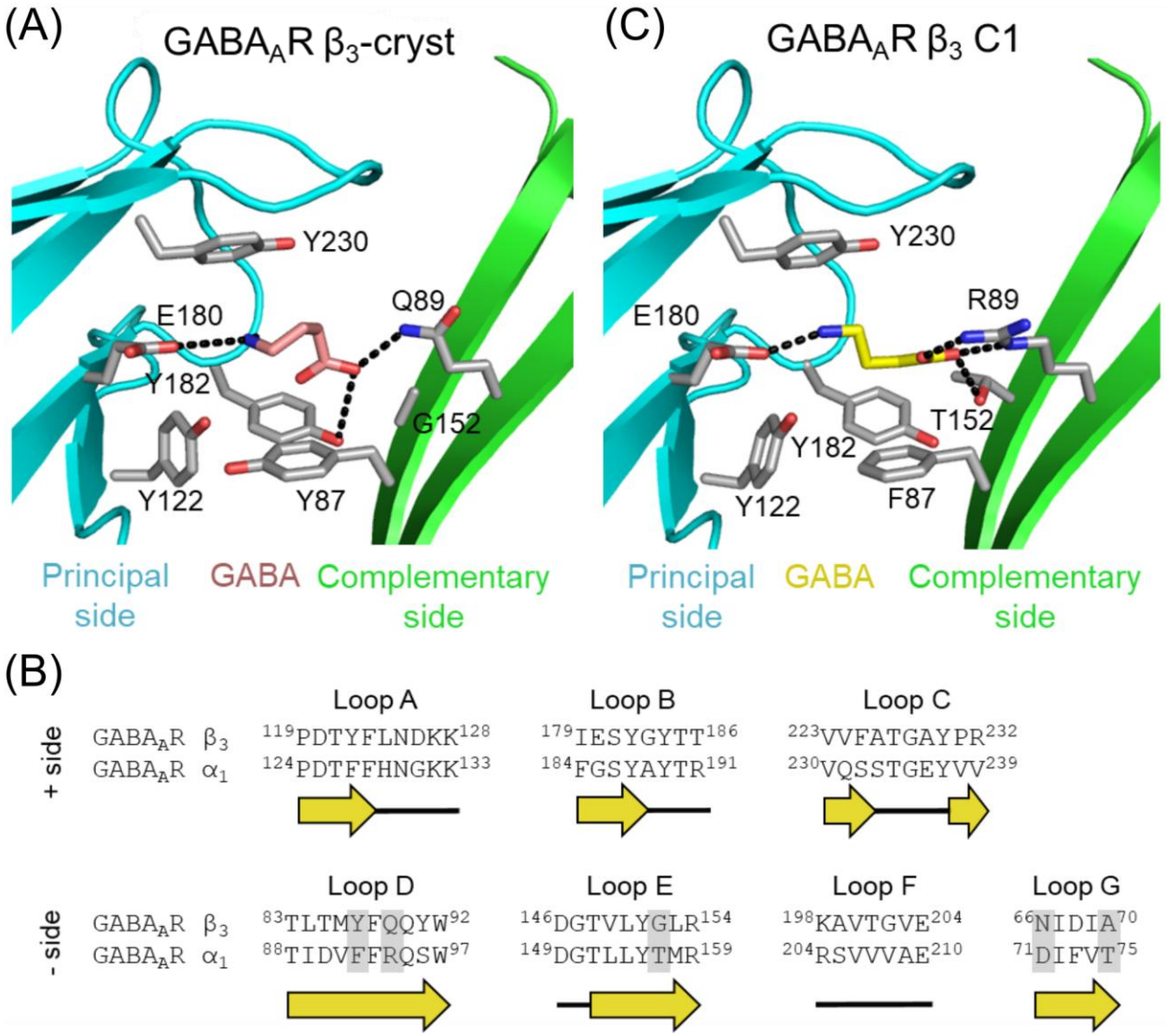

Figure 1. Docking results for $GABA_AR$ constructs. The predicted GABA orientations (pink and yellow) in (A) $GABA_AR$ β$_3$-cryst and (C) $GABA_AR$ β$_3$ C1 show the carboxyl group facing the complementary side (green cartoon) and the amino group facing the principal side (cyan cartoon). Residues interacting with GABA are depicted as grey sticks and polar interactions as black dashes. (B) Sequence alignment of the orthosteric site (loops A-G) based on structural comparisons of $GABA_AR$ β$_3$ (PDBID: 4COF) and $GABA_AR$ α$_1$ model (21), showing the substitutions (grey box). Secondary structure depicted below the sequence: loops (black line) and β-strands (yellow arrows). Residues are numbered according to the initiating Met1.

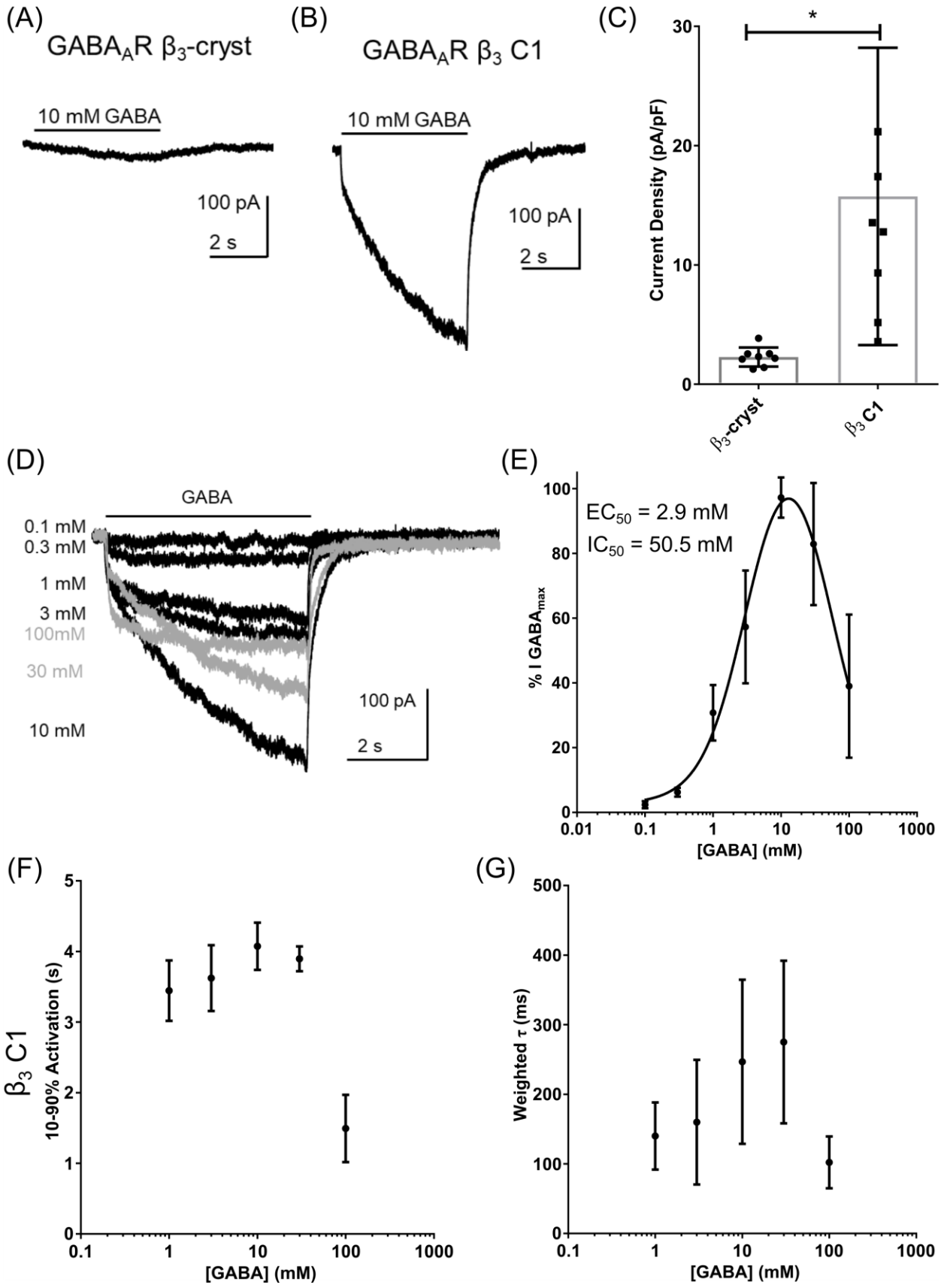
(A)
GABA$_A$R β$_3$-cryst
10 mM GABA
100 pA
2 s
(B)
GABA$_A$R β$_3$ C1
10 mM GABA
100 pA
2 s
(C)
*
Current Density (pA/pF)
30
20
10
0
β$_3$-cryst
β$_3$ C1
(D)
GABA
0.1 mM
0.3 mM
1 mM
3 mM
100mM
30 mM
10 mM
100 pA
2 s
(E)
EC$_{50}$ = 2.9 mM
IC$_{50}$ = 50.5 mM
% I GABA$_{max}$
100
80
60
40
20
0
0.01
0.1
1
10
100
1000
[GABA] (mM)
(F)
β$_3$ C1
10-90% Activation (s)
5
4
3
2
1
0
0.1
1
10
100
1000
[GABA] (mM)
(G)
Weighted τ (ms)
500
400
300
200
100
0
0.1
1
10
100
1000
[GABA] (mM)

Figure 2. $GABA_AR$ β_3 C1 is activated and inhibited by GABA. (A-B) Examples of currents recorded when GABA (10 mM) was applied to cells expressing (A) $GABA_AR$ β_3-cryst and (B) $GABA_AR$ β_3 C1 indicate that the latter is functional and activated by the neurotransmitter. (C) Mean ± SD current densities evoked by GABA (10 mM), showing significant differences between the proteins (n = 7, P = 0.003, t-test). (D) Examples of currents mediated by $GABA_AR$ β_3 C1, evoked by increasing concentrations of GABA. Currents in grey are declining due to inhibition by GABA (> 10 mM). The bar indicates GABA application (5 s). (E) Concentration-response relationships obtained using the percentage of the maximum amplitude recorded for each cell (n = 5). Logistic equations were fitted to the data points (see Experimental Procedures). From the double logistic fit, two distinct potencies were observed for activation (EC_{50} = 2.9 mM) and inhibition (IC_{50} = 50.5 mM). A summary of the data is in Table 2. (F) Graph of mean current 10-90% rise time. Activation rates are slowed somewhat by increasing the GABA concentration in β_3 C1 (n = 6, F (4,25) = 42.2, one-way ANOVA *post hoc* Dunnett's, *P* = 0.04 comparing 10 mM to 1 mM GABA), while currents evoked by 100 mM GABA activated faster (n = 6, *P* < 0.0001, F (4,25) = 42.2, one-way ANOVA *post hoc* Dunnett's, comparing 100 mM to 1 mM GABA). (G) Values for weighted τ of deactivation exhibited a similar trend with increasing GABA concentration (*P* = 0.04, one-way ANOVA, n = 6, F (4,19) = 3.2), although there was no significant difference comparing 1 mM to the other GABA concentrations tested. Detailed information about the components is in Table 3.

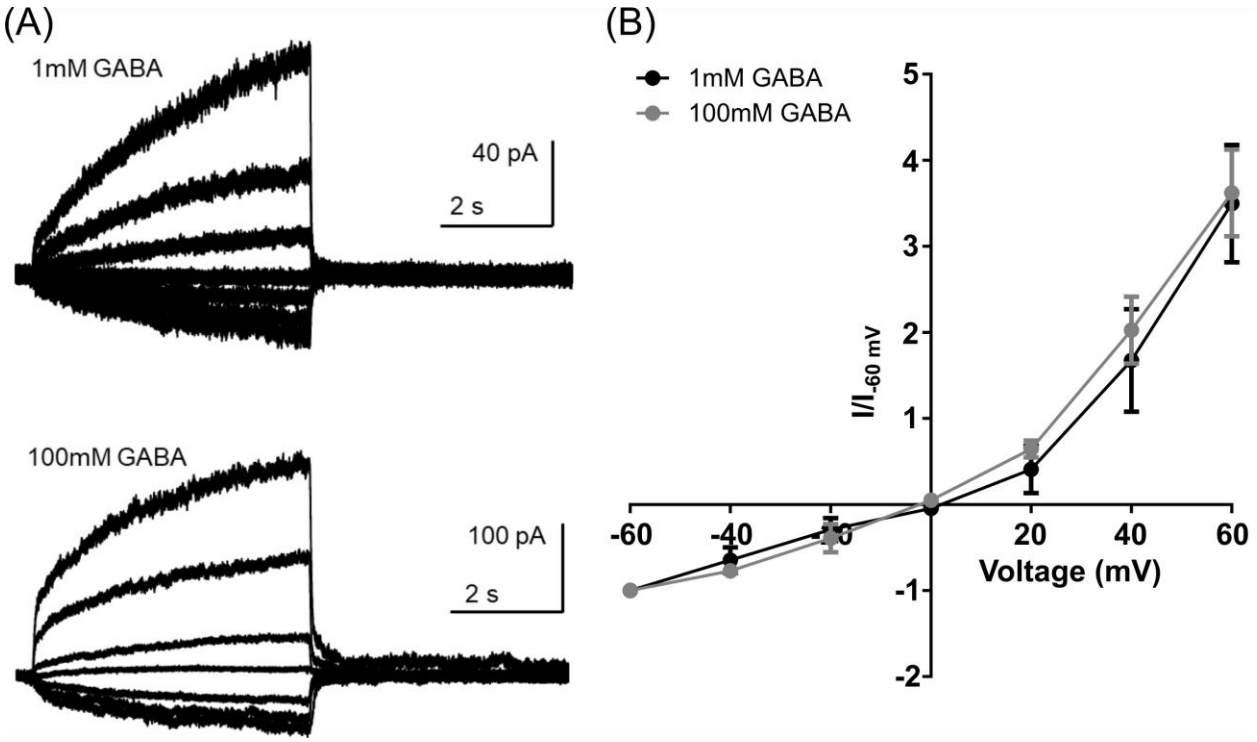

Figure 3. GABA does not block the channel by a voltage-dependent process. (A) Representative examples of the currents evoked by GABA (1 mM and 100 mM) recorded at voltages ranging from -60 mV to 60 mV. (B) The amplitude of the currents was expressed as a ratio of those evoked at -60 mV (I/I-60 mV) and plotted against the voltage, indicating similar outward rectification for both concentrations.

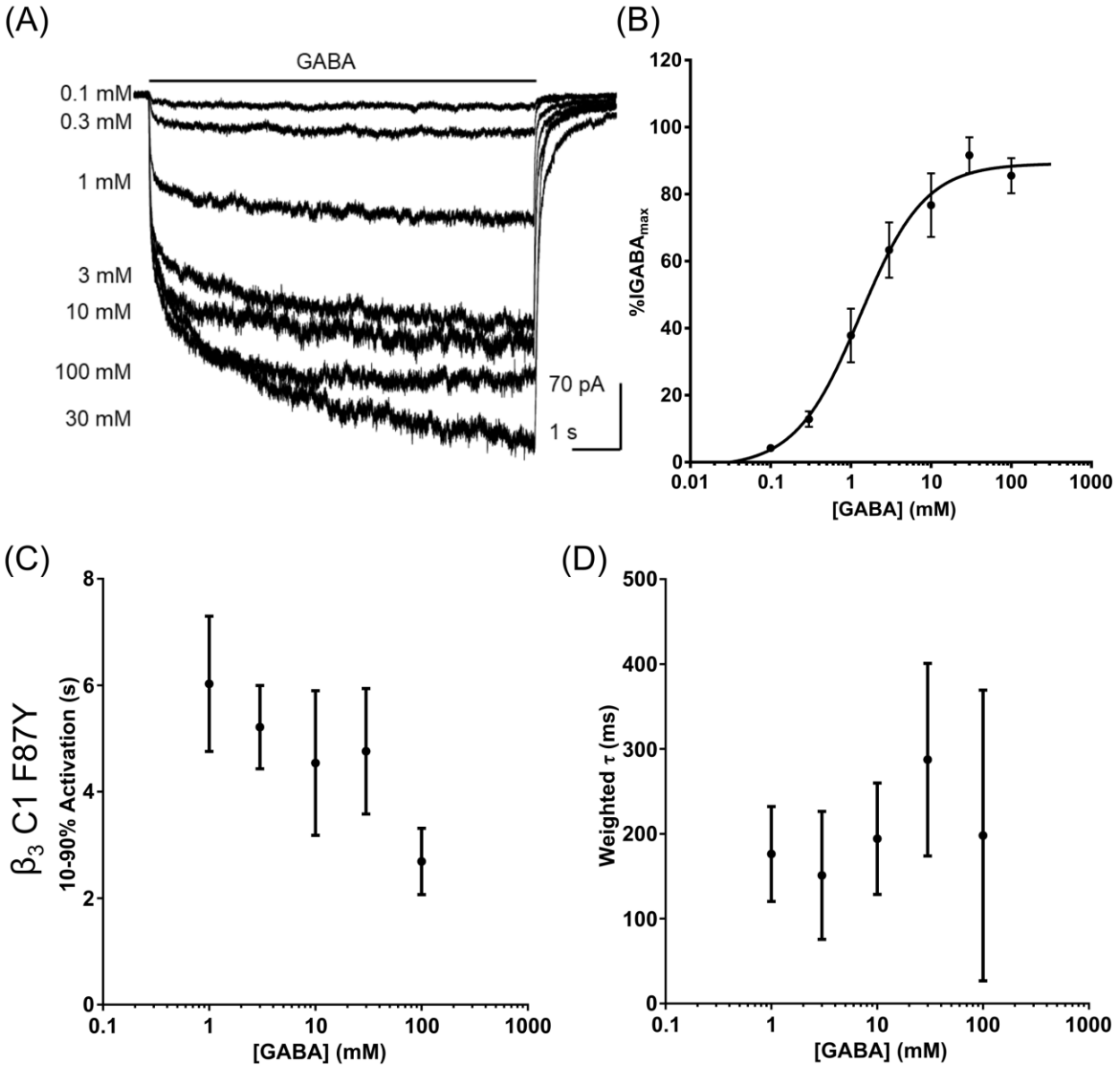

Figure 4. The C1 F87Y substitution abolished the biphasic nature of concentration-response relationship. (A) Examples of currents mediated by $GABA_AR$ β_3 C1 F87Y, evoked by increasing concentrations of GABA. (B) Concentration-response relationship obtained using the percentage of the maximum amplitude recorded for each cell. The inhibition caused by 100 mM GABA in β_3 C1 was abolished by the F87Y substitution. A summary of the data is in Table 2. (C) Mean 10-90% rise times showed no significant change with increasing GABA concentrations in β_3 C1 F87Y, except comparing 100 mM to 1 mM (P = 0.008, n = 4, F (4,15) = 5.2, one-way ANOVA *post-hoc* Dunnett's). (D) Mean deactivation weighted τ was also independent of GABA concentrations, (P = 0.5, one-way ANOVA, F (4, 15) = 0.96). Detailed information about the components is in Table 3.

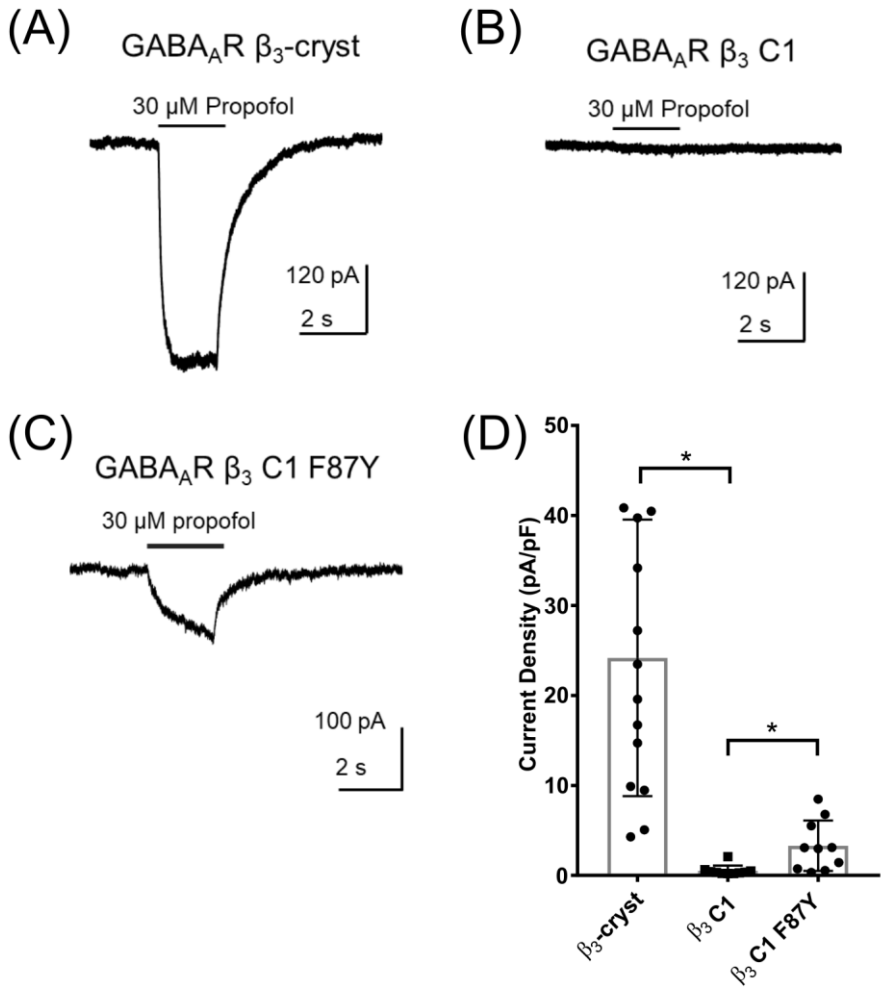

Figure 5. Propofol does not activate β_3 C1. Examples of currents recorded in the presence of propofol from HEK293 cells expressing (A) β_3-cryst, (B) β_3 C1 and (C) β_3 C1 F87Y. (D) Mean ± SD current densities evoked by propofol (30 μM) demonstrate the function of β_3 C1 is impaired, with values significantly different from the β_3-cryst (n = 10, *t*-test, β_3 C1: $P < 0.0001$). However, propofol direct activation was partially restored in β_3 C1 F87Y, with values significantly different from β_3 C1 (n = 10, $P = 0.007$, *t*-test).

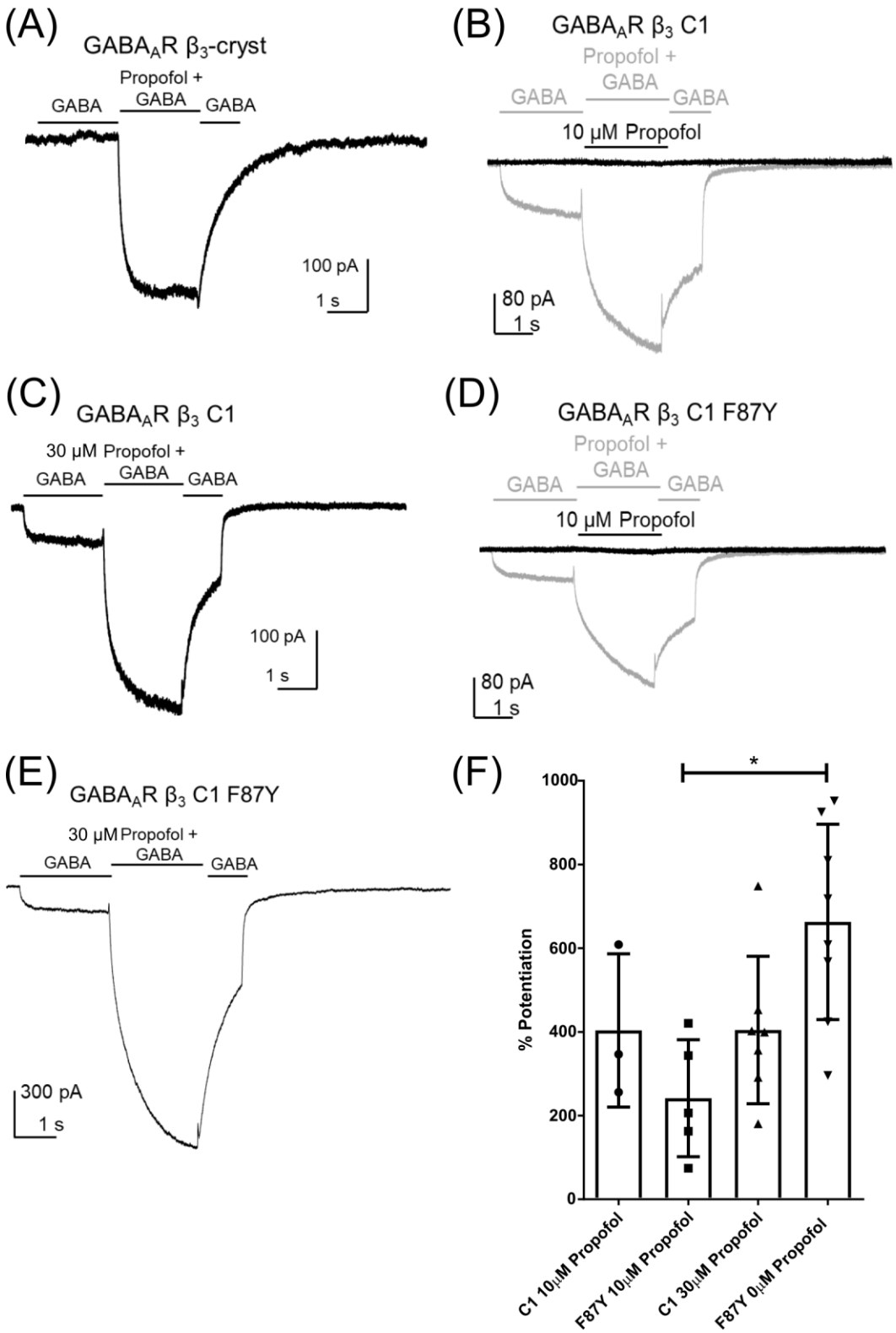

Figure 6. Potentiation of GABA-evoked currents by propofol was unaffected in the β_3 mutants. (A) An exemplar current evoked by propofol mediated by β_3-cryst. GABA had no effect and the current amplitude evoked by propofol is similar to that seen in the absence of GABA. Examples of GABA (1mM)-evoked currents mediated by β_3 C1 enhanced in the presence of (B) 10 μM propofol and (C) 30

μM propofol. Examples of GABA (1mM)-evoked currents mediated by β_3 C1 F87Y enhanced in the presence of (D) 10 μM propofol and (E) 30 μM propofol. (F) The percentage of potentiation by propofol at 10 μM and 30 μM, for β_3 C1 and β_3 C1 F87Y, were plotted, showing a significant difference for β_3 C1 F87Y between 10 μM and 30 μM propofol (n = 4, P = 0.008, F (3,19) = 5.3, one-way ANOVA *post hoc* Tukey's). This difference can be explained by the additive effect of propofol (30 μM) activation of β_3 C1 F87Y (Figure 5C). The bars indicate application of GABA (1 mM) or propofol (30 μM and 10 μM) with GABA (1 mM).